Scanning tunneling microscopy of ultrathin indium intercalated between graphene and SiC using confinement heteroepitaxy

Van Dong Pham[1*], César González[2,3], Yannick J. Dappe[4], Chengye Dong[5], Joshua A. Robinson[5,6,7,8], Achim Trampert[1], Roman Engel-Herbert[1]

[1]*Paul-Drude-Institut für Festkörperelektronik, Leibniz-Institut im Forschungsverbund Berlin e. V., Hausvogteiplatz 5-7, 10117 Berlin, Germany*

[2]*Departamento de Física de Materiales, Universidad Complutense de Madrid, E-28040 Madrid, Spain*

[3]*Instituto de Magnetismo Aplicado UCM-ADIF, Vía de Servicio A-6, 900, E-28232 Las Rozas de Madrid, Spain*

[4]*SPEC, CEA, CNRS, Université Paris-Saclay, Gif-sur-Yvette Cédex 91191, France*

[5] *Two-dimensional Crystal Consortium, Materials Research Institute, The Pennsylvania State University, University Park, Pennsylvania 16802, United States*

[6] *Department of Materials Science and Engineering, The Pennsylvania State University, University Park, Pennsylvania 16802, United States*

[7]*Department of Physics, The Pennsylvania State University, University Park, Pennsylvania 16802, United States*

[8]*Department of Chemistry, Materials Research Institute, The Pennsylvania State University, University Park, Pennsylvania 16802, United States*

*pham@pdi-berlin.de

ABSTRACT

Large-scale and air-stable two-dimensional metal layers intercalated at the interface between epitaxial graphene and SiC offer an appealing material for quantum technology. The atomic and electronic details as well as the control of the intercalated metals within the interface remain however very limited. In this Letter, we explored ultrathin indium confined between graphene and SiC using cryogenic scanning tunneling microscopy, complemented by first-principle density functional theory. Bias-dependent imaging and tunneling spectroscopy visualize a triangular superstructure with a periodicity of 14.7±3 Å and an occupied state at about -1.6 eV, indicating proof of highly crystalline indium. The STM tip was used to manipulate the number of indium layers below graphene, allowing to identify three monoatomic In layers and to tune their corresponding electronic properties with atomic precision. This further allows us to attribute the observed triangular superstructure to be solely emerged from In trilayer, tentatively explained by the lattice mismatch induced by lattice relaxation in the topmost In layer. Our findings provide a microscopic insight into the structure and electronic properties of intercalated metals within the graphene/SiC interface and a unique possibility to manipulate them with atomic precision using scanning probe technique.

Two-dimensional (2D) indium (In) has attracted great interest because it exhibits unusual physical properties such as a quantum spin Hall insulator **[1–3]**, extraordinary nonlinear optical response **[4]**, a nearly-free 2D electron gas system **[5]**, and a superconductor **[6]**, etc, that can be exploited as a compelling platform for fundamental research and quantum technology. In such context, confinement heteroepitaxy (CHet) has recently been introduced as a facile approach to prepare 2D In stabilized at the interface between epitaxial graphene (EG) and semiconductor SiC **[7]**. CHet uses homogeneous intercalation controlled by the incorporation of point defects into a fully covered monolayer graphene/SiC **[8]** to produce large-scale intercalated epitaxial In layers. Considering at atomic level, many important specifications of the CHet indium imposed by the graphene/SiC interface have not yet been explored. Moreover, flexible modulation in structure and electronic properties of the In with high accuracy exhibits a non-trivial challenge. Tuning the metal's layers has been only demonstrated by adjusting the amount of metal precursor **[9]**. Here, we used scanning tunneling microscopy (STM) complemented by density functional theory (DFT) to reveal structural details and electronic properties of intercalated In between graphene and SiC. In connection with our previous work **[10]** in which monolayer In was transformed into a bilayer using the STM tip, here, we converted a trilayer to a bilayer In and tuned the corresponding electronic properties. This demonstrates a practical advantage toward exploring and controlling the intercalated metal at the EG/SiC interface at the atomic level.

Intercalated In samples were prepared using CHet. Pristine EG was grown on a 6H-SiC (0001) as described elsewhere **[7]** and was exposed to O_2-plasma using a plasma generator (Tepla M4L) under a pressure of 500 mTorr with 150 sccm O_2 and 50 sccm He, and a 50 W power for 60s to generate point defects. The treated EG was heated up to 800^{o}C with In precursor for 30 min. After the intercalation was completed, the intercalated samples were transported in air, and degassed at 150^{o}C under ultra-high vacuum (UHV) before starting STM measurements. To ensure intercalation, we initially investigated In samples using different techniques before STM measurements which reflects ~90% trilayer and bilayer intercalated In as presented in Fig. S1.

Our measurements were carried out in a cryogenic STM system (Createc) operating at 5 K in UHV. The STM/STS were obtained using electrochemically etched tungsten tips which were carefully calibrated on an Ag (111) substrate. Differential conductance (dI/dV, I: tunneling current, V: voltage) was recorded using a lock-in technique with a bias modulation of 5 mV (peak-to-peak) and a modulation frequency of 675 Hz.

DFT calculations were performed using localized orbital basis set DFT code Fireball **[11]** that uses a self-consistent version of the LDA-like Harris-Foulkes functional **[12,13]**. The self-consistency of the electronic structure calculation was achieved using the occupation numbers. Optimized numerical basis sets have been used for In, C, Si and H with respective cutoff radii in atomic units of s=7.0, p=7.0 for In, s=4.5, p=4.5 for C **[14]**, s=4.8, p=5.4 for Si, and s=4.1 for H. We considered a 4×4-unit cell of graphene on top of a five-layer SiC slab, intercalated by one (1ML), two (2ML), or three (3ML) In monolayers. We used only one graphene layer in the simulation since the strongest interaction lies between In and SiC with a minimal contribution from the first graphene layer due to van der Waals interaction and a second graphene layer would not contribute any effect to the obtained results as it would be more than 6 Å away from the In layer. Consequently, we calculated the projected density of states (PDOS) of graphene and In.

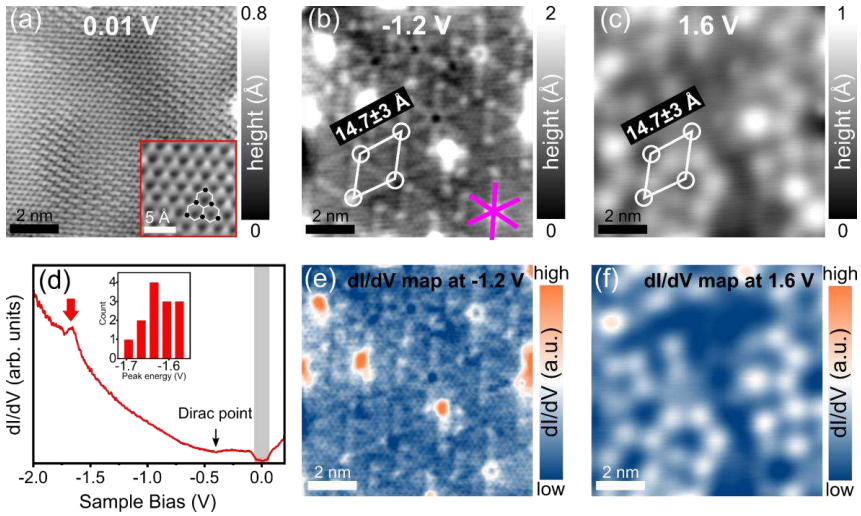

Fig. 1. *(a) STM topography image of EG/In/SiC at 0.01 V (1 nA). Inset: close-up STM image (0.01 V, 1 nA) revealing a "triangular-like" structure of graphene bilayer, guided by black dots. (b) STM image at -1.2 (1 nA) of the same area in (a). A low-pass filter was applied in (b) for a better observation of the superstructure. Purple lines indicate the graphene's armchair directions. (c) STM image of the same area in (a) at 1.6 V (1 nA). (d) dI/dV spectrum taken on EG/In/SiC*

revealing a phonon-inelastic induced gap (shaded rectangle), the Dirac point (black arrow), and an occupied peak at about -1.6 eV (red arrow). Inset: histogram of occupied peak position over different locations. (e-f) dI/dV maps taken at the same bias voltages used in (b) and (c), respectively.

At low bias voltage (0.01 V), the EG/In/SiC surface displays only the atomic resolution of the graphene honeycomb lattice as shown in Fig. 1(a). In comparison with a non-intercalated monolayer EG/SiC, where a 6×6 reconstruction is revealed in the low-bias STM images **[15–17]**, EG/In/SiC displays a smooth surface throughout all the probed locations indicating In intercalation. It is well-known that during intercalation, metal atoms reach the interface through the graphene defects **[18,19]** and interact with the sp^3 hybridized C atoms of the underlying graphene buffer layer (GBL) produced during the initial Si sublimation. At this point, they neutralize the remaining C-Si covalent bonds between the GBL and the SiC substrate **[20]**, transforming it into a new graphene layer and forming a bilayer graphene cap **[21,22]**. The high-resolution STM image in the inset of Fig. 1(a) shows a "triangular-like" atomic arrangement (see black dots), evident for a Bernal stacking in a graphene bilayer in which only the carbon atoms of one sublattice of the toplayer are imaged **[23]**.

Strikingly, point defects with various topographic symmetries are still observed in the graphene toplayer (see Fig. S2, supplementary material), identifying microscopic details of defect engineering used in CHet as defects are assumed to be healed during the intercalation at high temperatures **[7]** and is complementary to our recent observation of defects in monolayer EG/SiC **[8]**.

Imaging the same surface area in Fig. 1(a) at different bias voltages, we identified a triangular superstructure with a periodicity of 14.7±3 Å (see white rhombus) at -1.2 V shown in Fig. 1(b). We found this triangular pattern in all the probed locations despite different intercalation levels uncovered by other investigation techniques as shown in Fig. S1, supplementary material. We note that the pattern lines are only measured of ~2 pm and align with the armchair directions of the graphene indicated by purple lines (lower right). This superstructure is only visible in the filled-state images probed between -0.4 V and -1.6 V (see Fig. S3, supplementary material). In strong contrast, it is absent in the empty-state images obtained at 1.6 V, which reveals bright protrusions as shown in Fig. 1(c). The size and the nearest spacing between the protrusions are much larger

than the lattice parameters expected for monolayer In. By superimposing the filled-state and empty-state images, we found that the nodal points (white circles) created by intersecting the triangular pattern lines in Fig. 1(b) maintain the same positions as seen in Fig. 1(c). This indicates that the triangular pattern and the bright protrusions are structurally relevant. The dI/dV maps recorded at -1.2 and 1.6 V in Fig. 1(e) and Fig. 1(f), respectively, share similar features with their corresponding topographies, proving that these structures arise from the intercalated In. We rule out any structural relevance of the SiC observed here since the 6×6 reconstruction originated from GBL of SiC below a monolayer EG exhibits a constant periodicity of ~18 Å **[16]**. It is noted that individual In atoms were not resolved as previously measured in monolayer **[10,24,25]**. Therefore, our intercalated In sample might be composed of more than one monolayer and the observed triangular superstructure strongly indicates evidence of either lattice mismatch between different atomic planes or of quasi-surface reconstruction of the third In layer weakly bonded to EG. This uncertainty will be further discussed below. Nevertheless, the observation of this superstructure provides important experimental proof that the intercalated In has formed a highly crystalline structure between EG and SiC. In addition, the bright and dark spots seen in Fig. 1(b) reflect an inhomogeneity of the In layers, likely induced by impurities and vacancies **[25]**, leading to a large variation (±3 Å) in the superstructure periodicity.

dI/dV tunneling spectra, which are proportional to the local density of states (LDOS), were used to probe the EG/In/SiC electronic structures, identifying an occupied state and an n-doping of the EG. The spectrum in Fig. 1(d) measured on the EG/In/SiC captures the graphene LDOS reflected by a phonon-induced inelastic gap (shaded rectangle) and a Dirac point identified as a minimal depth at ~-0.4 eV below the Fermi level (E_F). The statistic of this Dirac point is represented in Fig. S4, supplementary material. This downshift indicates that the intercalated In acts as an electron donor to graphene, similar to other intercalated metal elements **[7,9,26]**. Note that the Dirac point of a bilayer EG on SiC is known to be around -0.31 eV **[17]** and is not observed here. The dominance of the graphene LDOS around E_F implies that the In atoms do not strongly interact with graphene. Probing towards large negative and positive biases revealed a pronounced occupied peak around -1.6 eV. This peak, marked by the red arrow in Fig. 1(d), varies when measured in different locations (see the inset), again indicating an inhomogeneity of the 2D In layers. This state is originally different from that of pristine and plasma-treated EG/SiC **[27,28]**,

and of SiC **[1]**, hence can be identified as a spectroscopic feature of the In, consistent with the *out-of-plane* p_z-derived In orbitals probed around the Γ point of the Brillouin zone **[1,3]**.

To obtain a more quantitative understanding of the intercalated In and explain the origin of the triangular superstructure, we performed tip-induced manipulation. As depicted schematically in Fig. 2(a), a bias voltage pulse of 8V was applied to the tip-sample junction above the EG/In/SiC for a few seconds (tip tunneling parameter: 2 V, 10 pA) while the tip height was simultaneously lowered until the tunneling current signal is saturated. The corresponding STM image in Fig. 2(b) reveals a significantly modified surface area below the tip as a deep crater with atomic steps fully exposed. This proves that the bias voltage pulse has locally altered the 2D metal, hence modifying the EG/SiC interface.

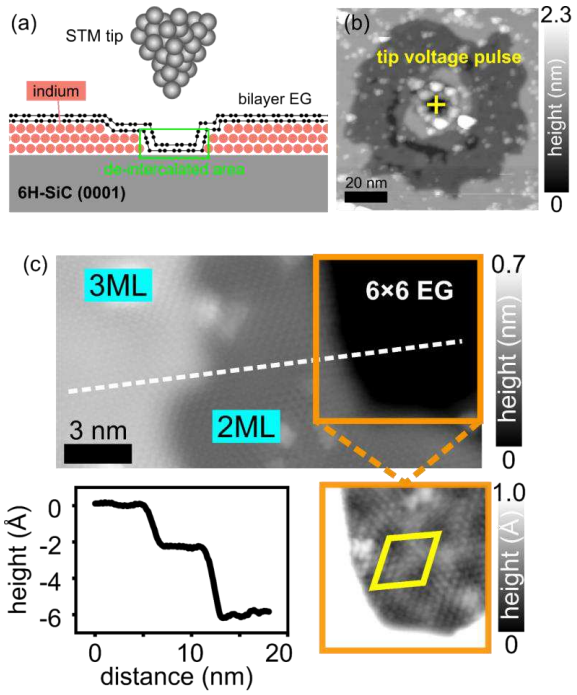

Fig. 2. *(a) Schematic of tip-induced manipulation on EG/In/SiC. (b) Large-scale STM image (2 V, 10 pA) of an area after applying an 8V voltage pulse to the tip-sample junction. (c) Upper: closed-up STM image (0.01 V, 1 nA) of an area upon tip-induced manipulation: three distinctive terraces are marked by 3ML (trilayer), 2ML (bilayer), and 6×6 EG (EG/SiC without intercalated In). Lower-left: height profile along the white dashed line in the upper image. Lower-right: STM image (0.01 V, 1 nA) of the 6×6 reconstruction of the lowest area.*

At a smaller length scale, we identified three atomic steps marked by trilayer (3ML), bilayer (2ML), and 6×6 EG in Fig. 2(c), upper panel. The height profile displayed in the lower left panel taken along the white dashed line represents the thicknesses of 3ML and 2ML regions with respect to the lowest 6×6 EG area: ~6 and ~4 Å, respectively. The lowest area marked as 6×6 EG (orange square) exhibits a 6×6 periodicity as a fingerprint of EG/SiC without intercalated metal (lower right panel) and is attributed to a *de-intercalated* area where In atoms were fully pushed away. Importantly, the graphene remains intact as it continuously covers the step edges as visible in Fig. 2(c), upper image. Considering ~2 Å to be the thickness of monolayer In at the EG/SiC interface **[4,10,24,25]**, we qualitatively attribute ~6 and ~4 Å to stem from In regions made of trilayer and bilayer, respectively. It is important to note that the 1ML region was not observed in our tip-induced experiments. The migration of In atoms below graphene is tentatively attributed to be either induced by the injection of energetic tunneling electrons from the tip through the inelastic tunneling process **[29–32]**, or other electric field-induced phenomena that is currently under investigation. This shows that the STM tip can be used to manipulate the metal layers at the EG/SiC interface with monolayer precision in conjunction with our recent work **[10]**.

It is further remarkable that the triangular superstructure is absent in the 2ML area but remains intact in the 3ML. This is evident in Fig. 3(a) and its Laplace-filtered STM image in Fig. 3(b). This observation indicates that the superstructure is only formed in the 3ML region, which is reinforced by the fact that the bias-dependent images taken on the 2ML area, marked by the green rectangle in Fig. 3(b), do not reveal any periodic structure (see Fig. S5, supplementary material). Note that defects are seen in bilayer and trilayer regions with more or less the same concentration, confirming that the triangular pattern is robust and unaffected by the defects. To a first approximation, we tentatively hypothesize that the superstructure is formed due to epitaxial strain at the In-SiC interface on the basis of the *in-plane* lattice mismatch between In and SiC. This strain

is finally released in the third In layer, leading to a larger In lattice spacing. As a consequence, the triangular pattern is the result of the superpositions induced by the lattice mismatch between two triangle lattices with different lattice constants (more detail can be found in Fig. S6, supplementary material) **[33]**. This is further supported by the absence of the superstructure in the 2ML regions (still coherently strained) after tip manipulation.

Modifying the number of In layers leads to a modulation in their DOS. Figure 3(c) shows two dI/dV spectra taken on the 3ML and 2ML terraces shown in Fig. 3(a). As the number of layers reduces from three to two, the occupied state significantly shifts from ~-1.6 to ~-1.2 eV, consistent with the previous observation **[3]**. The width of the latter peak is larger than the former, implying a stronger metal-substrate coupling in a bilayer than in a trilayer. This observation further proves that the occupied state originates only from In and its DOS can be controlled by tuning the number of layers.

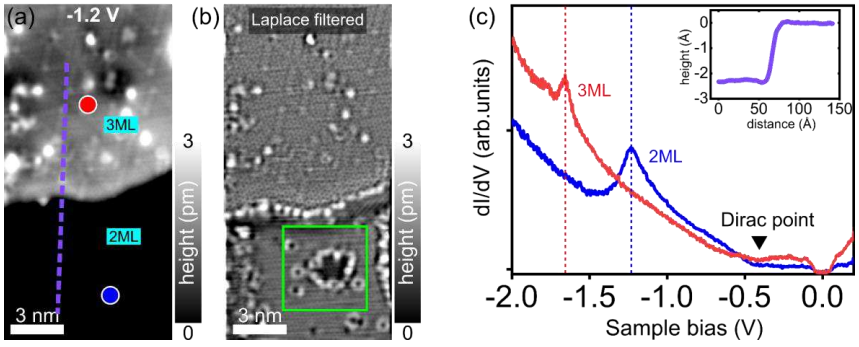

Fig. 3. *(a) A surface region upon tip-induced manipulation composed of 3ML and 2ML (-1.2 V, 0.2 nA). (b) Same area in (a) but Laplace-filtered. The green square marks the area for bias-dependent imaging measurement in Fig. S5. (c) dI/dV spectra measured on 3ML (red curve) and 2ML (blue curve) terraces revealing a shift of the occupied state. Inset: height profile of purple dashed line crossing 3ML and 2ML terraces.*

To further understand the structural and electronic properties of intercalated In, we carried out DFT calculations. We have considered 1ML, 2ML, and 3ML intercalated In between graphene

and SiC. The fully optimized structures are represented respectively in Fig. 4(a), (b), and (c). We found that In atoms in a monolayer can match in either a 1:1 or 1:√3 ratio above the topmost Si atoms of SiC, consistent with the experimental findings **[4,7,10,24,25]**. In contrast, bilayer and trilayer only adopt stable structures in a 1:1 registry (see Fig. S7, supplementary material). As the number of layers increases, they grow in an AA (bilayer) and AAA (trilayer) stacking as the energetically most favorable configuration which is partly in agreement with the cross-sectional scanning transmission electron microscopy (STEM) measurement: an AB and AAA stacking are visible for a bilayer and trilayer, respectively, as shown in Fig. S1(e), supplementary material. Note that no lattice deviation was found in the third In layer by DFT since the *in-plane* lattice parameter was fixed by the lattice vectors of the unit cell and applied for all the planes to avoid inducing complicated distortions inside the cells. We found an In-In distance of 3.10 Å (in-plane) for all configurations and 2.80/2.90 Å (out-of-plane) for In bilayer/trilayer. The In-Si distance is found to be ~2.65 Å for all configurations, revealing a strong coupling with Si, while the In-C distance is ~3.20 Å, corresponding to the van der Waals interaction.

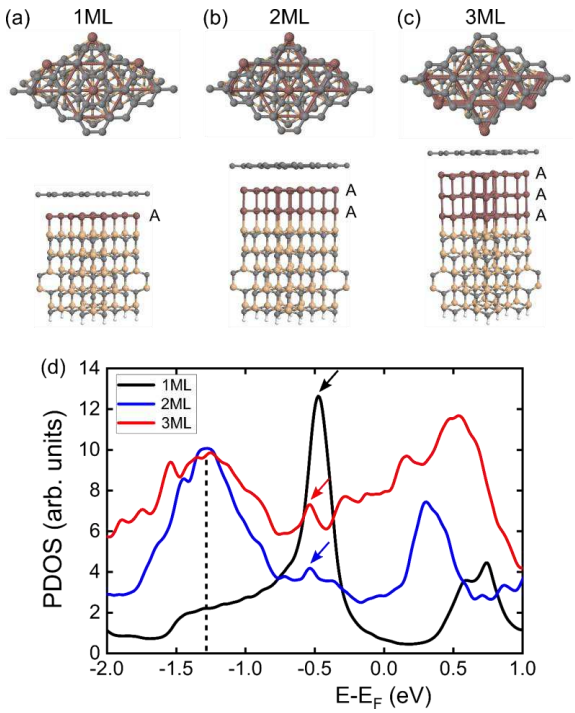

Fig. 4. (a-c) Top and side view of fully relaxed In structures for 1, 2, and 3ML intercalated between EG and SiC. Note that In layers grow in AA (2ML) and AAA (3ML) stacking above the Si atoms. (d) Corresponding In PDOS for each configuration. An intense peak (arrows) at -0.5 eV is observed for 1ML (black curve), and strongly reduced in 2ML (blue) and 3ML (red). A peak around -1.3 eV (dashed line) only for 2ML and 3ML is in good agreement with experiments.

We have calculated the electronic structures of the three In configurations as presented in Fig. 4(d). As it can be seen, for 1ML, a strong peak at around -0.5 eV below E_F is present which significantly reduces in intensity in 2ML and 3ML (see arrows), suggesting that 1ML In strongly interacts either with the SiC substrate or in a minor term with graphene. As shown in Fig. S8, supplementary material, the peak at -0.5 eV is also present in the graphene PDOS in EG/In/SiC and absent in bilayer and trilayer In. This implies that the peak at -0.5 eV may have emerged from a strong In-SiC or In-graphene hybridization. In the cases of 2ML and 3ML, this peak is strongly

reduced, which indicates a remarkable decoupling of In from the SiC. We observed a peak at around -1.3 eV (dashed line) in the 2ML and 3ML arising from the derived In orbitals, in good agreement with experiment observation. However, this peak does not shift when going from 2ML to 3ML as experimentally observed in Fig. 3(c). This discrepancy most likely originates from the different stackings between the experiment (AB), verified by the STEM data in Fig. S1(e) and the DFT calculation (AA).

In conclusion, cryogenic scanning tunneling microscopy and spectroscopy in combination with DFT calculation have been used to identify the details of the structure and electronic properties of ultrathin In intercalated at the EG/SiC interface prepared by CHet. The STM tip was used as a unique tool to access the metal layers and to manipulate them with monoatomic layer precision, allowing us to tune their electronic properties. Our work introduces a promising approach for understanding and manipulating the properties of intercalated metals at the interface between graphene and SiC with atomic precision beyond the currently known approaches.

SUPPLEMENTARY MATERIAL

See the supplementary material for more details on sample characterization and demonstration which support the discussion in the main text.

The authors thank M. Hanke (Paul-Drude-Institut für Festköperelektronik) for critical reading of the manuscript, and S. Fölsch (Paul-Drude-Institut für Festköperelektronik) for the technical supports and discussions. We acknowledge the computer resources at Altamira and the technical support provided by IFCA of the University of Cantabria (FI-2023-1-0016). We thank H. Wang for preparing STEM cross-sectional samples via focused ion beam (FIB) and K. Wang for STEM support. J. A. Robinson and C. Dong are supported by 2DCC-MIP under NSF cooperative agreement DMR-2039351 and the Materials Research Science and Engineering Center for Nanoscale Science through the NSF Grant DMR-2011839.

AUTHOR DECLARATIONS

Conflict of Interest

The authors have no conflicts to disclose

Author contributions

Van Dong Pham: STM investigation; Analysis; Writing – original manuscript; Writing – review & editing. **César González** and **Yannick J. Dappe**: DFT calculations; Writing – review & editing. **Chengye Dong** and **Joshua A. Robinson:** Analysis; Writing – review. **Achim Trampert:** Analysis; Writing – review & editing. **Roman Engel-Herbert:** Review.

DATA AVAILABILITY

The data that supports the findings of this study are available within the article [and its supplementary material].

REFERENCES

[1] M. Bauernfeind, J. Erhardt, P. Eck et al. *Design and Realization of Topological Dirac Fermions on a Triangular Lattice*, Nat Commun 12, 5396 (2021).

[2] C. Schmitt, J. Erhardt, P. Eck et al. *Achieving Environmental Stability in an Atomically Thin Quantum Spin Hall Insulator via Graphene Intercalation*, Nat Commun 15, 1486 (2024).

[3] J. Erhardt, M. Bauernfeind, P. Eck et al. *Indium Epitaxy on SiC(0001): A Roadmap to Large Scale Growth of the Quantum Spin Hall Insulator Indenene*, J. Phys. Chem. C 126, 16289-16296 (2022).

[4] M. A. Steves, Y. Wang, N. Briggs et al. *Unexpected Near-Infrared to Visible Nonlinear Optical Properties from 2-D Polar Metals*, Nano Lett. 20, 8312-8318 (2020).

[5] E. Rotenberg, H. Koh, K. Rossnagel et al. *Indium 7 × 3 on Si(111): A Nearly Free Electron Metal in Two Dimensions*, Phys. Rev. Lett. 91, 246404 (2003).

[6] S. Yoshizawa, H. Kim, Y. Hasegawa et al. *Disorder-Induced Suppression of Superconductivity in the Si (111) − (7 × 3)-In Surface: Scanning Tunneling Microscopy Study*, Phys. Rev. B 92, 041410 (2015).

[7] N. Briggs, B. Bersch, Y. Wang et al. *Atomically Thin Half-van Der Waals Metals Enabled by Confinement Heteroepitaxy*, Nat. Mater. 19, 637-643 (2020).

[8] V. D. Pham, C. González, Y. J. Dappe et al. *Atomic-Scale Characterization of Defects in Oxygen Plasma-Treated Graphene by Scanning Tunneling Microscopy*, Carbon 227, 119260 (2024).

[9] S. Forti, S. Link, A. Stöhr et al. *Semiconductor to Metal Transition in Two-Dimensional Gold and Its van Der Waals Heterostack with Graphene*, Nat Commun 11, 2236 (2020).

[10] V. D. Pham, C. Dong, and J. A. Robinson, *Atomic Structures and Interfacial Engineering of Ultrathin Indium Intercalated between Graphene and a SiC Substrate*, Nanoscale Adv. 5, 5601-5612 (2023).

[11] J. P. Lewis, P. Jelínek, J. Ortega et al. *Advances and Applications in the FIREBALL Ab Initio Tight-Binding Molecular-Dynamics Formalism*, Phys. Status Solidi B 248, 1989–2007 (2011).

[12] J. Harris, Y. J. Dappe, P. Jelínek et al. *Simplified Method for Calculating the Energy of Weakly Interacting Fragments*, Phys. Rev. B 31, 1770 (1985).

[13] W. M. C. Foulkes and R. Haydock, *Tight-Binding Models and Density-Functional Theory*, Phys. Rev. B 39, 12520 (1989).

[14] M. A. Basanta, Y. J. Dappe, P. Jelínek et al. *Optimized Atomic-like Orbitals for First-Principles Tight-Binding Molecular Dynamics*, Computational Materials Science 39, 759-766 (2007).

[15] G. M. Rutter, N. P. Guisinger, J. N. Crain et al. *Imaging the Interface of Epitaxial Graphene with Silicon Carbide via Scanning Tunneling Microscopy*, Phys. Rev. B 76, 235416 (2007).

[16] C. Riedl, U. Starke, J. Bernhardt et al. *Structural Properties of the Graphene-SiC(0001) Interface as a Key for the Preparation of Homogeneous Large-Terrace Graphene Surfaces*, Phys. Rev. B 76, 245406 (2007).

[17] P. Lauffer, K. V. Emtsev, R. Graupner et al. *Atomic and Electronic Structure of Few-Layer Graphene on SiC (0001) Studied with Scanning Tunneling Microscopy and Spectroscopy*, Phys. Rev. B 77, 155426 (2008).

[18] Y. Liu, X. Liu, C-Z. Wang et al. *Mechanism of Metal Intercalation under Graphene through Small Vacancy Defects*, J. Phys. Chem. C 125, 6954−6962 (2021).

[19] X. Lu, Y. Liu, M. Shao et al. *Defect-Mediated Intercalation of Dysprosium on Buffer Layer Graphene Supported by SiC(0001) Substrate*, Chemical Physics Letters 742, 137162 (2020).

[20] K. V. Emtsev, A. A. Zakharov, C. Coletti et al. *Ambipolar Doping in Quasifree Epitaxial Graphene on SiC(0001) Controlled by Ge Intercalation*, Phys. Rev. B 84, 125423 (2011).

[21] C. Riedl, C. Coletti, T. Iwasaki et al. *Quasi-Free-Standing Epitaxial Graphene on SiC Obtained by Hydrogen Intercalation*, Phys. Rev. Lett. 103, 246804 (2009).

[22] S. Link, S. Forti, A. Stöhr et al. *Introducing Strong Correlation Effects into Graphene by Gadolinium Intercalation*, Phys. Rev. B 100, 121407 (2019).

[23] G. M. Rutter, J. N. Crain, N. P. Guisinger et al. *Structural and Electronic Properties of Bilayer Epitaxial Graphene*, Journal of Vacuum Science & Technology A: Vacuum, Surfaces, and Films 26, 938–943 (2008).

[24] T. Hu, D. Yang, W. Hu et al. *The Structure and Mechanism of Large-Scale Indium-Intercalated Graphene Transferred from SiC Buffer Layer*, Carbon 171, 829-836 (2021).

[25] H. Kim, N. Tsogtbaatar, B. Tuvdendorj et al. *Effects of Two Kinds of Intercalated In Films on Quasi-Free-Standing Monolayer Graphene Formed above SiC (0001)*, Carbon 159, 229-235 (2020).

[26] P. Rosenzweig and U. Starke, *Large-Area Synthesis of a Semiconducting Silver Monolayer via Intercalation of Epitaxial Graphene*, Phys. Rev. B 101, 201407 (2020).

[27] F. Hiebel, P. Mallet, L. Magaud et al. *Atomic and Electronic Structure of Monolayer Graphene on 6 H -SiC (000 1 ¯) (3 × 3) : A Scanning Tunneling Microscopy Study*, Phys. Rev. B 80, 235429 (2009).

[28] T. Hu, D. Yang, H. Gao et al. *Atomic Structure and Electronic Properties of the Intercalated Pb Atoms underneath a Graphene Layer*, Carbon 179, 151-158 (2021).

[29] T.-C. Shen, C. Wang, G. C. Abeln et al. *Atomic-Scale Desorption Through Electronic and Vibrational Excitation Mechanisms*, Science 268, 1590-1592 (1995).

[30] R. S. Becker, G. S. Higashi, Y. J. Chabal et al. *Atomic-Scale Conversion of Clean Si (111):H-1×1 to Si (111)-2×1 by Electron-Stimulated Desorption*, Phys. Rev. Lett. 65, 1917 (1990).

[31] J. W. Lyding, T.-C. Shen, J. S. Hubacek el at. *Nanoscale Patterning and Oxidation of H-passivated Si (100)-2×1 Surfaces with an Ultrahigh Vacuum Scanning Tunneling Microscope*, Appl. Phys. Lett. 64, 2010–2012 (1994).

[32] K. T. He, J. D. Wood, G. P. Doidge et al. *Scanning Tunneling Microscopy Study and Nanomanipulation of Graphene-Coated Water on Mica*, Nano Lett. 12, 2665−2672 (2012).

[33] A. Ohtake, X. Yang, and J. Nara, *Structure and Morphology of 2H-MoTe2 Monolayer on GaAs(111)B Grown by Molecular-Beam Epitaxy*, Npj 2D Mater Appl 6, 35 (2022).